Electro-optical processor for measuring displacement employing the Talbot and the nonsteady-state photo-electromotive force effects

P. Rodriguez-Montero,* D. Sánchez-de-la-Llave, and S. Mansurova

National Institute for Astrophysics, Optics and Electronics A.P. 51, Puebla 72000, Mexico
*Corresponding author: ponciano@inaoep.mx

We present a device for measuring displacement based on the Talbot and the nonsteady photo-electromotive force effects. The proposed device does not require any numerical signal processing since its output signal is, in appropriate regions, linearly related to the measured displacement. The proposed system requires an illuminating field with a sinusoidal amplitude distribution and low fringe visibility. The dynamic range can be adjusted according to the illuminating field spatial period or wavelength. Displacements with an estimated resolution better than 10 µm in a dynamic range of 1.5 mm were detected using a sinusoidal amplitude grating with a period $d = 100$ µm.   © 2013 Optical Society of America

OCIS codes: (050.1950) Diffraction gratings; (070.6760) Talbot and self-imaging effects; (120.1088) Adaptive interferometry; (160.5140) Photoconductive materials.
http://dx.doi.org/10.1364/OL.39.000104

The near-field diffraction of a periodic object has the special property of repeating itself in intensity at certain propagation distances; this effect is widely known as the Talbot effect [1–3]. In particular, when an amplitude transmittance that is periodic along one axis is illuminated by a monochromatic plane wave, the field distribution at the transmittance plane repeats itself at multiples of the so called Talbot distance. The Talbot distance depends only on two parameters, namely, the illuminating wavelength (λ) and the transmittance spatial period (d). More precisely, for plane wave illumination, the Talbot distance is given by $Z_T = 2d^2/\lambda$. The field intensity in planes between Talbot distances remains periodic, although not necessarily with the same period as that of the transmittance.

Here we consider the simplest case of a one-dimensional sinusoidal amplitude grating, which can be described by

$$t(x) = \frac{1}{2}\left[1 + m\,\cos\left(\frac{2\pi x}{d}\right)\right],\qquad(1)$$

where d is the grating period and m is the grating modulation index. In the near-field and under plane-wave illumination, the field intensity distribution at the axial distance z from the grating plane is given by

$$I(x,z) = \frac{1}{4}\left[\begin{array}{c}1 + 2m\,\cos\left(\frac{2\pi z}{Z_T}\right)\cos\left(\frac{2\pi x}{d}\right)\\ + m^2\cos^2\left(\frac{2\pi x}{d}\right)\end{array}\right].\qquad(2)$$

For low values of the grating modulation index ($m \ll 1$), it is straightforward to show that the fringe visibility (V) for the intensity pattern described by Eq. (2) can be expressed as

$$V(z) \cong \left|2m\,\cos\left(\frac{2\pi z}{Z_T}\right)\right|.\qquad(3)$$

Hence, by measuring the fringe visibility at an observation plane of interest, the distance between the sinusoidal amplitude grating and the desired observation plane can be unambiguously determined in a distance range of one fourth the Talbot distance, e.g., from $z = 0$ to $z = Z_T/4$.

The Talbot effect has been exploited in the past for several metrological applications, among them the measurement of the refractive index [4], the measurement of temperature [5], contouring [6], the measurement of focal length [7], collimation testing [8], wavefront sensors [9], and the measurement of distance and displacement [10–14]. For this latter application, the first proposal [10] relied on measuring the fringe contrast or visibility (V) of the diffracted field intensity and realizing temporal processing of the detected images. Afterward, Schirripa Spagnolo and Ambrosini proposed a measurement method that used either a cosine [11] or a Ronchi [12] grating and then realized numerical Fourier processing of the detected intensity pattern to determine the distance between the grating and the observation plane. Finally, methods for measuring discrete distances using the Talbot effect were proposed by Metha *et al.* [13] and Dubey *et al.* [14]. In [13], two wavelengths were employed to measure a step-height that coincides with the difference between the Talbot distances associated with each of the wavelengths utilized. In [14] a superluminescent diode was employed to provide several wavelengths instead of two. In all of the proposals mentioned above, the fields of interest were detected by a CCD camera and numerical processing of the detected images was required in order to determine its visibility and hence, the propagation distance.

On the other hand, Rodriguez-Montero *et al.* [15] demonstrated the use of detectors based on the nonsteady-state photo-electromotive force (photo-emf) effect for assisted Talbot interferometry.

In this work, we demonstrate a detection scheme to measure the displacement of a mirror-like object which combines the Talbot effect with the photo-emf-based

detector. The information about displacement is codified in the visibility of the diffracted field; however, in contrast to the previous proposals, the decodification is achieved by direct measurement of the photo-emf current without any image processing.

A detailed description of the detectors based on the photo-emf effect can be found in [16,17]. The effect consists in the generation of an electrical current through a short-circuited photo-conductor material when it is illuminated by a vibrating, spatially nonuniform light pattern. The current is the result of the spatial mismatch between the space charge electric field distribution (stored in the photoconductor impurity centers) and the photo-excited carriers' distribution. This current is known as the photo-emf current and the photo-conductive sample as the photo-emf detector. For the simplest case of a vibrating sinusoidal light pattern (with period d) illuminating the detector, the photo-emf current amplitude J^Ω can be written as

$$J^\Omega = CI_0 \delta V^2, \qquad (4)$$

where I_0 is the average intensity on the detector, δ is the amplitude of the vibrations, and the factor C depends on electro-optical parameters of the sample, as well as on the spatial (K) and temporal (Ω) frequencies of the illuminating pattern, which are fixed in our experiment. Equation (4) was obtained under the assumptions of low visibility ($V \ll 1$) of the light pattern and small amplitude of vibrations ($\delta \ll d$).

Now, if the light patterns are created by the sinusoidal amplitude grating described by Eq. (1), which is vibrating on the direction of its grating vector, then the axial dependence of the photo-emf current is obtained by substitution of Eq. (3) into Eq. (4):

$$J^\Omega(z) = 4m^2 CI_0 \delta \left\{ \frac{1}{2} + \frac{1}{2}\cos\left[\frac{2\pi z}{(Z_T/2)}\right] \right\}. \qquad (5)$$

From Eq. (5) it is evident that by measuring the photo-emf current, the distance between the vibrating sinusoidal amplitude grating and the detector can be determined. This property can be used for measuring the displacement of a mirror-like object as it is demonstrated in the following experiment. The detection scheme proposed by us is depicted in Fig. (1).

The input light field was generated by illuminating a quasi-sinusoidal amplitude grating (with a period $d = 100$ μm) with a collimated He–Ne laser beam ($\lambda = 633$ nm), so the theoretical value for the Talbot distance is 31.60 mm. A highly collimated beam is required since a curvature on the illuminating field will produce Talbot distances that are not equidistant [3]. In our experimental set up, the degree of collimation is such that it practically yields more than 15 equidistant self-image planes from the grating. The vibrations of the light patterns (with the frequency of 600 Hz) were produced by gluing the grating to a piezoelectric transducer. The amplitude of the vibrations measured by an accelerometer was about 15 μm, so the required condition for small δ is fulfilled. A beam splitter directs the beam to a mirror mounted on a translational stage and the back reflection from this
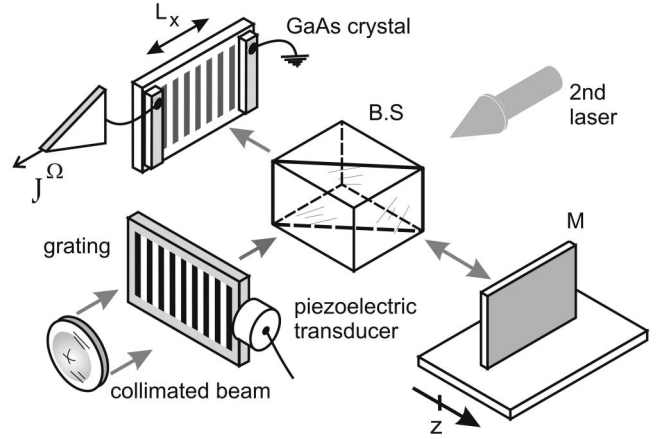

Fig. 1.   Experimental setup for measuring the displacements of a mirror-like object by the photo-emf detector. BS, beam splitter; M, mirror on a translation stage.

mirror is brought to the surface of a photo-emf detector. The electrical current generated by the detector is measured as a voltage drop across the impedance of the lock-in amplifier (100 MΩ, 25 pF). A second laser provides a background illumination to further decrease the visibility at the photo-emf detector plane.

The photo-emf detector was fabricated from a photoconductive GaAs crystal, with dimensions of 7×5 mm in the front surface and 0.5 mm in thickness. In the front surface, a pair of silver paint electrodes were deposited in such a way that the effective interelectrode surface was $L_X = 3$ mm and $L_Y = 5$ mm. The photo-emf detector was characterized by standard techniques [16,17], and it was found that the current depends linearly on the vibration amplitude δ and quadratically on the visibility V of a vibrating sinusoidal interference pattern as predicted by Eq. (4).

Figure (2) shows the output signal from the photo-emf detector as a function of the displacement of the mirror in steps of 250 μm. As predicted by the theory [Eq. (5)], the output signal varies as a cosine function of distance. Note that because of the geometry employed, the expected period of the cosine function is $Z_T/4$, and it agrees very well with the experimentally observed value
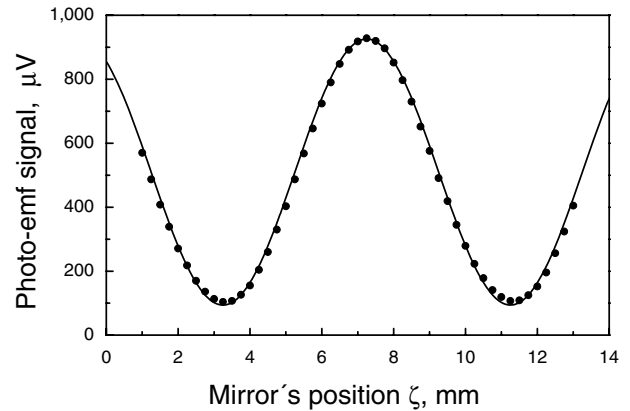

Fig. 2.   Experimental dependence of the photo-emf signal as a function of the mirror displacement. The light power impinging on the photo-emf detector from the grating is 0.52 mW and from the background is 0.36 mW. The fitting values are $V_0 = 510$ μV, $V_C = 416$ μV, and $Z_T/4 = 8$ mm.

$(8.0 \pm 0.5 \text{ mm})$ considering a sampling interval of $250 \, \mu\text{m}$. The maximum value of the photo-emf signal corresponds to a mirror's position such that the total distance traveled by the light from the grating plane to the photo-emf detector is equal to a multiple of $Z_T/2$ (11 Z_T in this particular experiment) where the visibility of the diffracted field is expected to be maximal (Eq. 5). The positions of minimal current, i.e., positions of minimal (nominally zero) visibility, correspond to total propagation distances equal to $10.75 Z_T$ and $11.25 Z_T$.

Note, however, that although Eq. (5) predicts a minimal current equal to zero, the experimental photo-emf signal is not zero. This is due to some contribution of high diffraction orders, which are present in the quasi-sinusoidal grating we employed and to the photo-emf detector response to the spatial frequency of the illuminating pattern [16,17]. Nevertheless, the minimal photo-emf signal can reach a value close to zero by increasing the background illumination but at the expense of reducing the signal maximal value.

The measured photo-emf signal V^Ω can be expressed as

$$V^\Omega = V_0 + V_C \cos\left(\frac{2\pi z}{Z_T/4}\right), \tag{6}$$

where V_0 is the offset and V_C is the amplitude of the sinusoidal component. The solid line in Fig. (2) is a fit to Eq. (6) with $V_0 = 510 \, \mu\text{V}$, $V_C = 416 \, \mu\text{V}$, and $Z_T/4 = 8$ mm.

As shown in Fig. (2) and stated in Eq. (5), around the total propagation distances equal to $z = ((2n + 1)/8)Z_T$, with $n = 0, 1, 2\ldots$; there is a region in which the output signal current from the photo-emf detector is linearly proportional to the mirror's displacement. Figure (3) shows the photo-emf signal around the mirror's position $\zeta = 5.25$ mm in steps of $20 \, \mu\text{m}$, where $n = 43$. The linear relationship is clearly demonstrated with a correlation coefficient of 0.999. This linear relationship holds in a range of about 1.5 mm. The photo-emf signal proved to be very stable and the measurements are quite reproducible, yielding a device with high precision, as far as the illuminating intensity and the piezoelectric vibration amplitude and frequency remain constant. Indeed, the fluctuations in the photo-emf signal are of the same order of the diameter of the dots representing the experimental data. From this plot it is clear t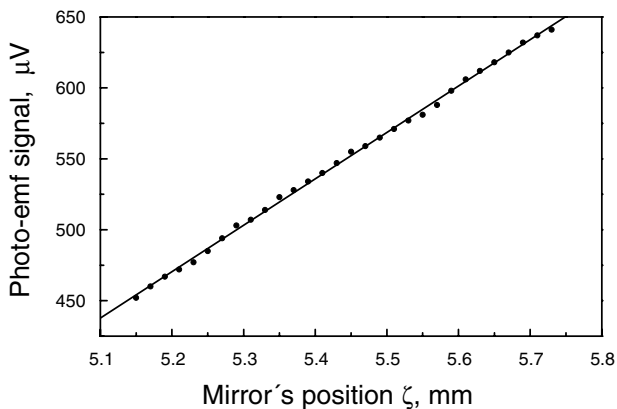hat under our experimental conditions, the proposed system can resolve displacements of the order of $10 \, \mu\text{m}$. The uncertainty in the mirror's position determined by the translation stage is $5 \, \mu\text{m}$.

The previous results were obtained employing a quasi-sinusoidal amplitude grating to generate the above described illuminating field; however, any technique that generates the described illuminating field can be used. We obtained similar results employing a Ronchi grating in order to generate a sinusoidal input field. In this case, we filtered the three central orders of a vibrating Ronchi grating spectrum. We carried out this filtering by reducing the diameter of the collimated beam in such a way that only the three central orders of the Ronchi grating spectrum were present at the interelectrode spacing of the photo-emf detector. The results obtained were very similar to the ones presented above.

Finally, it can be inferred from Eq. (6) and Fig. (2) that the dynamic range is proportional to the Talbot distance. Therefore, since the Talbot distance is given by $Z_T = 2d^2/\lambda$, the dynamic range of the device can be increased by increasing the grating period or by reducing the illuminating wavelength. However, a trade-off exists with the device resolution. On the one hand, increasing the dynamic range produces smaller changes in visibility for the same sampling interval. On the other hand, the smallest detectable change in the photo-emf current depends exclusively on the detector's characteristics. Hence, the device resolution is equal to the propagation distance that produces the minimum detectable change in the photo-emf current.

Summarizing, we have presented an electro-optical system capable of measuring displacement of mirror-like objects. The system design is based on the self-imaging phenomenon and the photo-emf effect. No numerical signal processing is required since the output signal current from the photo-emf detector is proportional to the square of the detected field visibility. Our proposal was verified using a GaAs photo-emf detector. In contrast to previously reported systems based on the Talbot effect, whose response time is limited by the image acquisition time and processing algorithms, the response time of our system is determined by the relaxation time of the photo-emf detector photo-conductive material, e.g., approximately 10^{-7} s for the crystal we employed. Two methods for generating a sinusoidal field were employed, obtaining very similar results. Since the Talbot distance is proportional to the ratio of the sinusoidal field period squared over the wavelength, the dynamic range can be modified by changing the grating period or by changing the illuminating wavelength, at the expense of modifying the device measurement resolution. Because of the inherent adaptive properties of the detectors based on the photo-emf effect, the proposed technique is very robust regarding environmental perturbations and vibrations. In the linear region of the dependence of the photo-emf signal as a function of the mirror displacement, an estimated resolution better than $10 \, \mu\text{m}$ in a dynamic range of 1.5 mm was demonstrated using a quasi-sinusoidal amplitude grating with a period $d = 100 \, \mu\text{m}$.

To the best of our knowledge, this is the first time that the Talbot effect is employed for measuring distance in an electro-optical processor that does not require numerical signal processing.

Fig. 3. Photo-emf signal around the mirror's position $\zeta = 5.25$ mm. The measurements were taken with a lock-in time constant of 1 s.

References

1. H. F. Talbot, Philos. Mag. **9**(56), 401 (1836).
2. L. Rayleigh, Philos. Mag. **11**, 196 (1881).
3. K. Patorski, Prog. Opt. **47**, 1 (1989).
4. J. C. Bhattacharya, Appl. Opt. **28**, 2600 (1989).
5. C. Shakher and A. J. Pramila Daniel, Appl. Opt. **33**, 6068 (1994).
6. P. Singh, M. S. Faridi, C. Shakher, and R. S. Sirohi, Appl. Opt. **44**, 1572 (2005).
7. S. Mirza and C. Shakher, Opt. Eng. **44**, 013601 (2005).
8. J. Dhanotia and S. Prakash, Appl. Opt. **50**, 1446 (2011).
9. D. Podanchuk, V. Kurashov, A. Goloborodko, V. Dańko, M. Kotov, and N. Goloborodko, Appl. Opt. **51**, C125 (2012).
10. P. Chavel and T. C. Strand, Appl. Opt. **23**, 862 (1984).
11. G. Schirripa Spagnolo and D. Ambrosini, Meas. Sci. Technol. **11**, 77 (2000).
12. G. Schirripa Spagnolo, D. Ambrosini, and D. Paoletti, J. Opt. A **4**, S376 (2002).
13. D. S. Metha, S. K. Dubey, C. Shakher, and M. Takeda, Appl. Opt. **45**, 7602 (2006).
14. S. K. Dubey, D. S. Metha, A. Roy, and C. Shakher, Opt. Commun. **279**, 13 (2007).
15. P. Rodríguez-Montero, C. M. Gómez-Sarabia, and J. Ojeda-Castañeda, Appl. Opt. **47**, 3778 (2008).
16. S. Stepanov, in *Handbook of Advanced Electronic and Photonics Materials and Devices*, H. S. Nalwa, ed. (Academic 2001) Vol **2**, pp. 205–272.
17. M. P. Petrov, I. A. Sokolov, S. I. Stepanov, and G. S. Trofimov, J. Appl. Phys. **68**, 2216 (1990).